



# Selective naked-eye detection of Magnesium (II) ions using a coumarin-derived fluorescent probe<sup>☆</sup>

Vinod Kumar Gupta<sup>a,b,\*</sup>, Naveen Mergu<sup>a</sup>, Lokesh Kumar Kumawat<sup>a</sup>, Ashok Kumar Singh<sup>a</sup>

<sup>a</sup> Department of Chemistry, Indian Institute of Technology Roorkee, Roorkee 247 667, India

<sup>b</sup> Department of Applied Chemistry, University of Johannesburg, Johannesburg, South Africa

## ARTICLE INFO

### Article history:

Received 16 August 2014

Received in revised form 6 October 2014

Accepted 10 October 2014

Available online 22 October 2014

### Keywords:

Chemosensor

Coumarin

Fluorescence

Naked-eye detection

Binding mode

## ABSTRACT

A simple 4-Methyl-7-hydroxy-8-formyl Coumarin (CS) serves as a selective chemosensor for  $\text{Mg}^{2+}$  in the presence of alkali and alkaline earth metal ions. It showed a significant fluorescence enhancement towards  $\text{Mg}^{2+}$ . The receptor CS exhibited a good binding constant and lowest detection limit for  $\text{Mg}^{2+}$ . The variation of emission signal exists via of reversible chelation enhanced fluorescence (CHEF) with this inherent quenching metal ion.

© 2014 Elsevier B.V. All rights reserved.

## 1. Introduction

Magnesium is the fourth most abundant cation in the human body, most abundant divalent cation within cells and plays an important physiological role in many of its functions [1]. Also magnesium found in the bone and plays an active role in bone remodelling and skeletal development [2,3]. On the other side, magnesium is the eighth most abundant element on earth crust [4]. Magnesium deficiency can result from a variety of causes including gastrointestinal and renal losses, can cause a wide variety of features including cardiac, hypokalaemia, hypocalcaemia and neurological manifestations. A number of chronic diseases, such as diabetes, osteoporosis, hypertension and coronary heart disease have been associated with chronic low magnesium [5,6]. Detection of  $\text{Mg}^{2+}$  in the presence of other alkali and alkaline earth metal ions, like as  $\text{Ca}^{2+}$ ,  $\text{Na}^{+}$  and  $\text{K}^{+}$  is of particular significance. Serum magnesium and the magnesium tolerance test are the most widely used. There are no easy and readily available methods to assess magnesium status.

The design of fluorescent chemosensors is an active field of research for analytical as well as environmental and biological problems [7–11]. Typically, chemosensors are small molecules and are able to bind selectively and reversibly the analyte of interest with a change in the sensing system property, such as absorption, emission and redox potentials, which may allow naked eye detection of the analyte without resorting to the use of any expensive instruments. Of the various kinds of chemosensors, the fluorescent based chemosensors present many advantages. Fluorescence measurements are usually very sensitive, low cost, easily performed, capability of real-time detection and versatile [12–17].

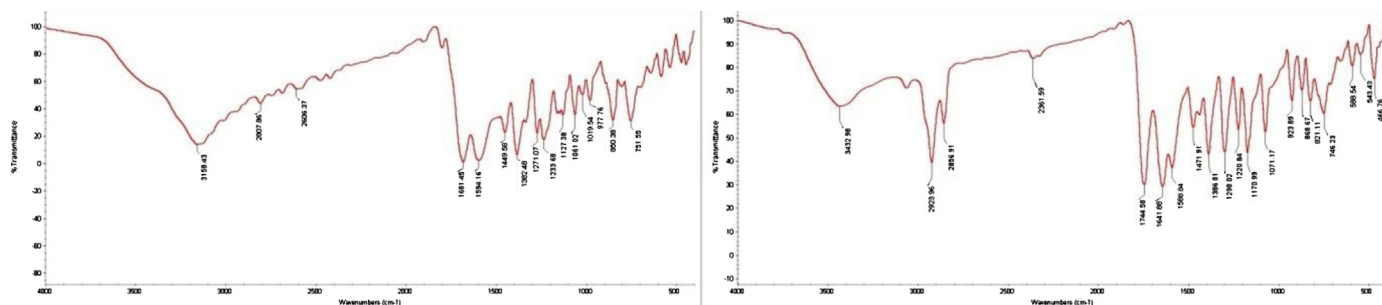
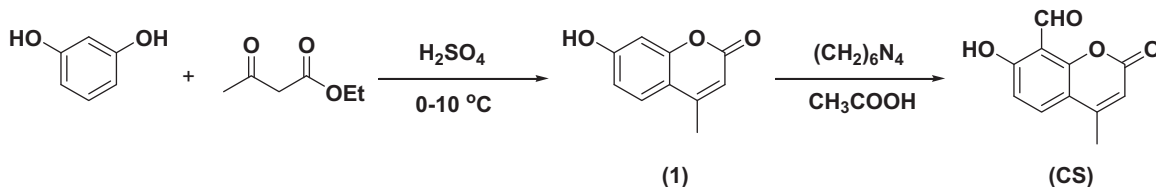
Till now, various families of fluorescent probes for  $\text{Mg}^{2+}$  have been developed. These probes have receptor groups based upon moieties including diaza-18-crown-6 [18], benzo-15-crown-5 [19], calix[4]arene [20], Benzo chromene [21], Imidazo-1,10-phenanthroline [22] and other [23–27]. Most of the reported fluorescent probes for  $\text{Mg}^{2+}$  demonstrate poor selectivity for  $\text{Mg}^{2+}$  over  $\text{Ca}^{2+}$  and are useful only where the  $\text{Mg}^{2+}$  ion concentrations are much higher than those of  $\text{Ca}^{2+}$  ion.

We now report the ability of 4-Methyl-7-hydroxy-8-formyl Coumarin (CS) as a fluorescent probe to serve as an effective chemosensor for  $\text{Mg}^{2+}$  in the presence of other alkali and alkaline earth metal ions. Our particular interest is to investigate how  $\text{Mg}^{2+}$  affects the fluorescent behaviour of fluorophore upon complexation.

<sup>☆</sup> Paper presented at the 7th European conference on Optical Sensors and Biosensors, Athens, Greece, 13–16 April 2014.

\* Corresponding author. Tel.: +91 1332285801; fax: +91 1332273560.

E-mail addresses: [vinodfcy@iitr.ac.in](mailto:vinodfcy@iitr.ac.in), [vinodfcy@gmail.com](mailto:vinodfcy@gmail.com) (V.K. Gupta).

Fig. 1. FT-IR Spectrum of **1** and **CS**.Scheme 1. Synthetic route for **CS**.

## 2. Experimental

### 2.1. Reagents and apparatus

All the commercially available chemicals were purchased from Merck and Aldrich and used without further purification. The IR spectra were recorded on a Nexus FT-IR (Illinois, USA) spectrometer in the range 4000–400  $\text{cm}^{-1}$  with KBr. The NMR spectra were measured by using Bruker 500 MHz (USA), TMS as an internal standard, DMSO- $d_6$ ,  $\text{CDCl}_3$  and  $\text{CD}_3\text{OD}$  are taken as solvents. The mass spectra were recorded on a Bruker-microTOF II (USA). The UV–vis absorption spectra were obtained on a Shimadzu UV-2450 spectrophotometer (Japan) and the Fluorescent spectra were recorded by using Shimadzu RF-5301PC spectrofluorophotometer (Japan). Differential Pulse Voltammetric experiments were performed using a CHI760E electrochemical workstation (USA) with a conventional three-electrode configuration consisting of a glassy carbon working electrode, a platinum wire counter electrode, and

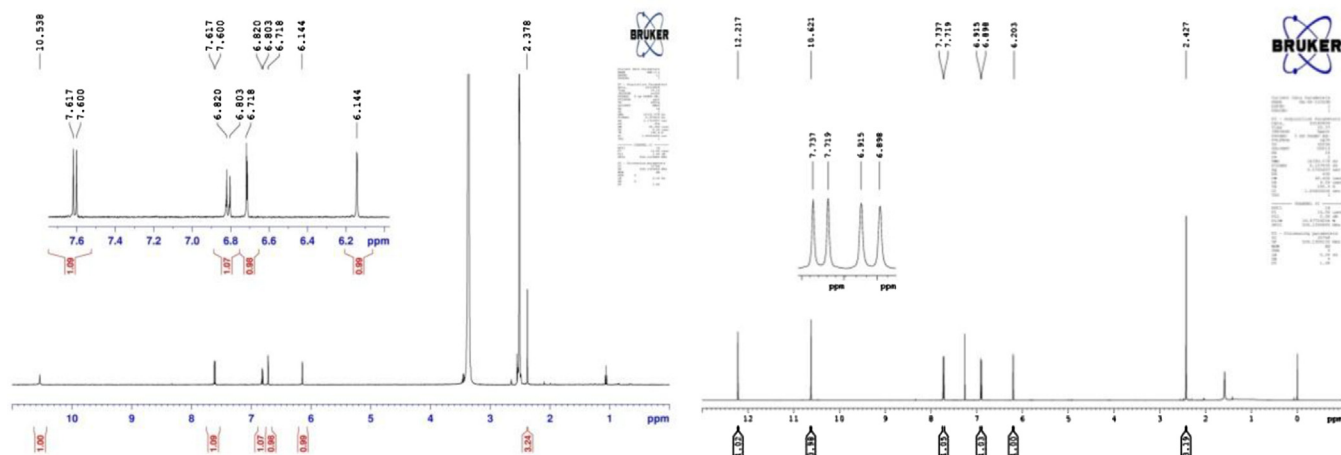
an aqueous  $\text{Ag}/\text{AgNO}_3$  reference electrode. The pH was measured with a Eutech CyberScan pH 510 (Singapore).

### 2.2. Synthesis and characterisation

The synthetic route of Chemosensor (**CS**) was outlined in Scheme 1. Chemosensor was prepared by following the literature method [28,29] and the structure was characterised by FT-IR,  $^1\text{H}$  NMR and HRMS spectra (Figs. 1–3).

#### 2.2.1. Synthesis of 4-Methyl-7-hydroxy Coumarin (**1**):

Concentrated sulphuric acid (20 mL) was cooled at 0–5  $^{\circ}\text{C}$  in an ice bath. A solution of resorcinol (20 mmol) in ethyl acetoacetate (30 mmol) was added to sulphuric acid under constant stirring at 0–5  $^{\circ}\text{C}$ . The reaction mass was stirred about 2–3 h under the same conditions and poured in to crushed ice under vigorous stirring. Obtained solid was filtered and recrystallised from

Fig. 2.  $^1\text{H}$  NMR Spectrum of **1** and **CS**.

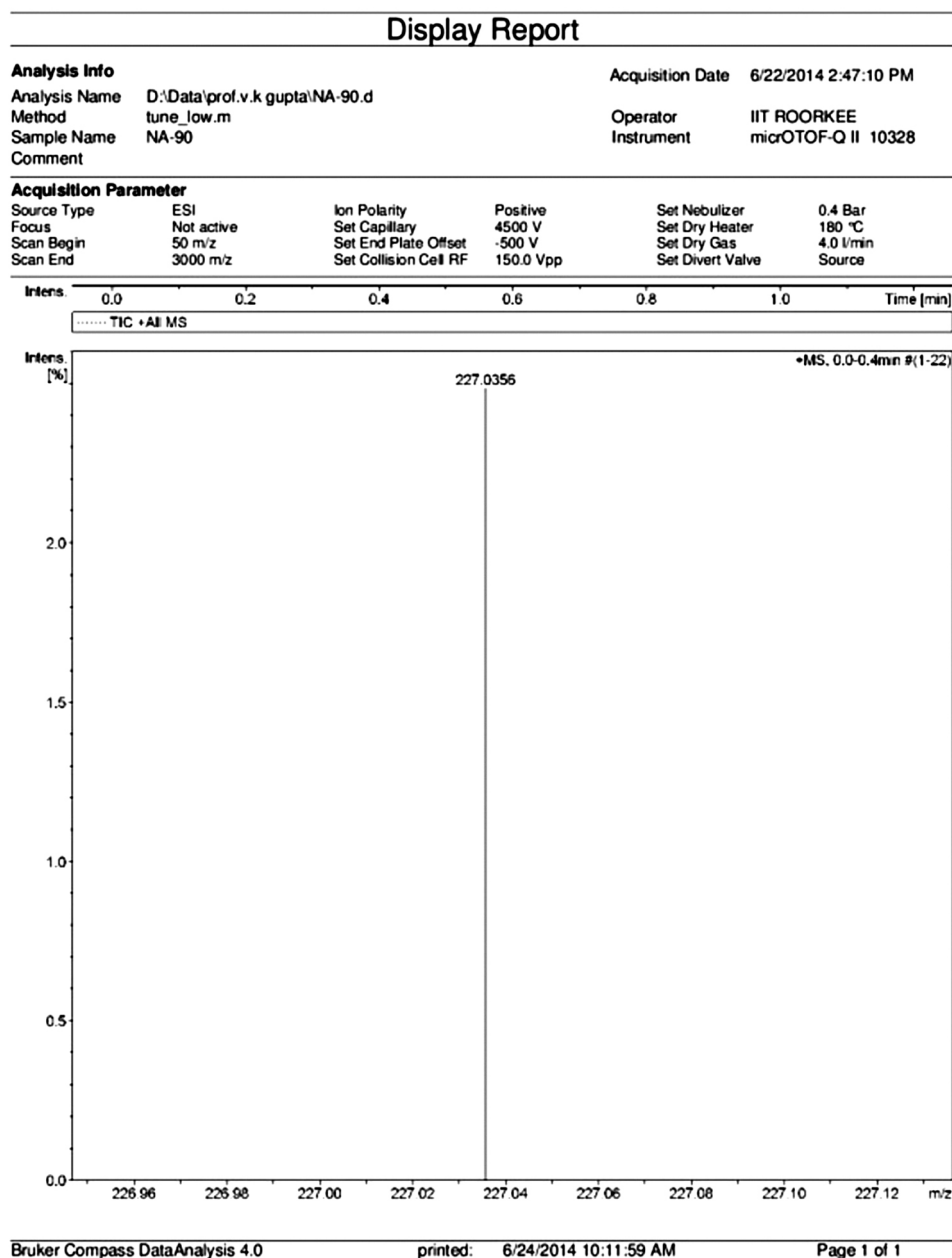


Fig. 3. HRMS Spectrum of CS.

methanol. Yield: 2.8 g (79%); color: White crystals; m.p. 179–181 °C; FT-IR (KBr),  $\nu$ ,  $\text{cm}^{-1}$ : 3158 (O–H), 1681 (C=O), 1594 (C=C), 1382, 1234 (C–O);  $^1\text{H}$  NMR (DMSO- $d_6$ ),  $\delta$ , ppm ( $J$ , Hz): 2.38 (s, 3H), 6.14 (s, 1H), 6.72 (s, 1H), 6.81 (d,  $J$ =8.5, 1H), 7.61 (d,  $J$ =8.5, 1H), 10.54 (s, 1H).

#### 2.2.2. Synthesis of 4-Methyl-7-hydroxy-8-formyl Coumarin (CS):

The mixture of 7-hydroxy-4-methyl-coumarin (10 mmol), hexamethylene tetramine (30 mmol) in glacial acetic acid (20 mL) was refluxed for 4–5 h in a water bath. Then, 20% HCl (25 mL) was added and further heated for 30 min, cooled to room temperature and extracted with diethyl ether. Solid was obtained on evaporation of solvent. Yield: 0.37 g (18%); color: pale yellow solid; m.p. 175–177 °C; FT-IR (KBr),  $\nu$ ,  $\text{cm}^{-1}$ : 3433 (O–H), 2924 (OC–H), 1745 (HC=O), 1642 (C=O), 1589 (C=C), 1387, 1298 (C–O);  $^1\text{H}$  NMR

( $\text{CDCl}_3$ ),  $\delta$ , ppm ( $J$ , Hz): 2.43 (s, 3H), 6.20 (s, 1H), 6.91 (d,  $J$ =8.5, 1H), 7.73 (d,  $J$ =9.0, 1H), 10.62 (s, 1H), 12.22 (s, 1H). ESI calcd for  $\text{C}_{11}\text{H}_8\text{O}_4$  ( $M + \text{Na}$ ) $^+$ : 227.0320, found: 227.0356.

#### 2.3. UV-vis and fluorescent studies

All measurements of UV-vis absorption and fluorescence emission spectra were carried out in 1.0 cm path length quartz cuvettes in alcoholic medium (MeOH) at room temperature. Absorption and emission spectra of the chemosensor in the presence of various metal ions were measured in the concentration of 50  $\mu\text{M}$  (for absorption spectra), 10  $\mu\text{M}$  (for emission spectra). Stoichiometry, binding constant of sensing probe– $\text{Mg}^{2+}$  complex and limit of detection of  $\text{Mg}^{2+}$  were calculated by using spectrofluorophotometer. For all the measurements, excitation wavelength was 350 nm,

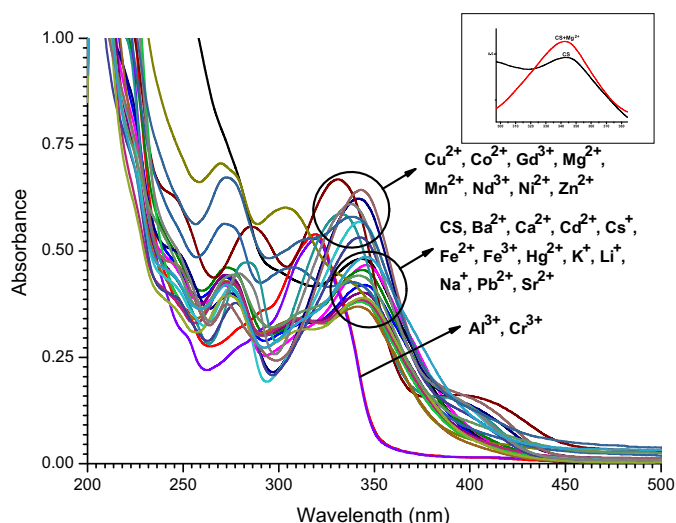


**Fig. 4.** UV-vis absorbance spectra of **CS** (50  $\mu\text{M}$ ) in the presence of 1.0 equiv. of various metal ions in MeOH.

and both the excitation and emission slit widths were 3 and 5 nm, respectively.

### 3. Results and discussion

The binding ability and mode of chemosensor towards  $\text{Mg}^{2+}$  were investigated through absorption, emission, electrochemical and  $^1\text{H}$  NMR spectroscopic experiments.

#### 3.1. Absorption spectroscopic studies

The binding ability of probe (50  $\mu\text{M}$ ) against cations (50  $\mu\text{M}$ ), such as  $\text{Al}^{3+}$ ,  $\text{Ba}^{2+}$ ,  $\text{Ca}^{2+}$ ,  $\text{Cd}^{2+}$ ,  $\text{Co}^{2+}$ ,  $\text{Cr}^{3+}$ ,  $\text{Cs}^+$ ,  $\text{Cu}^{2+}$ ,  $\text{Fe}^{2+}$ ,  $\text{Fe}^{3+}$ ,  $\text{Gd}^{3+}$ ,  $\text{Hg}^{2+}$ ,  $\text{K}^+$ ,  $\text{Li}^+$ ,  $\text{Mg}^{2+}$ ,  $\text{Mn}^{2+}$ ,  $\text{Na}^+$ ,  $\text{Nd}^{3+}$ ,  $\text{Ni}^{2+}$ ,  $\text{Pb}^{2+}$ ,  $\text{Sr}^{2+}$  and  $\text{Zn}^{2+}$  was carried out by UV-vis absorption spectroscopic studies in methanol. The free ligand **CS** exhibited a single absorption band at about 343 nm, hyperchromic shift was observed when added to  $\text{Co}^{2+}$ ,  $\text{Cu}^{2+}$ ,  $\text{Gd}^{3+}$ ,  $\text{Mg}^{2+}$ ,  $\text{Mn}^{2+}$ ,  $\text{Nd}^{3+}$ ,  $\text{Ni}^{2+}$  and  $\text{Zn}^{2+}$  ions (Fig. 4). It showed a blue shift accompanied by a hyperchromic shift in the presence of  $\text{Cr}^{3+}$  and  $\text{Al}^{3+}$  metal ions. The other cations  $\text{Ba}^{2+}$ ,  $\text{Ca}^{2+}$ ,  $\text{Cd}^{2+}$ ,  $\text{Cs}^+$ ,  $\text{Fe}^{2+}$ ,  $\text{Fe}^{3+}$ ,  $\text{Hg}^{2+}$ ,  $\text{K}^+$ ,  $\text{Li}^+$ ,  $\text{Na}^+$ ,  $\text{Pb}^{2+}$  and  $\text{Sr}^{2+}$  did not show

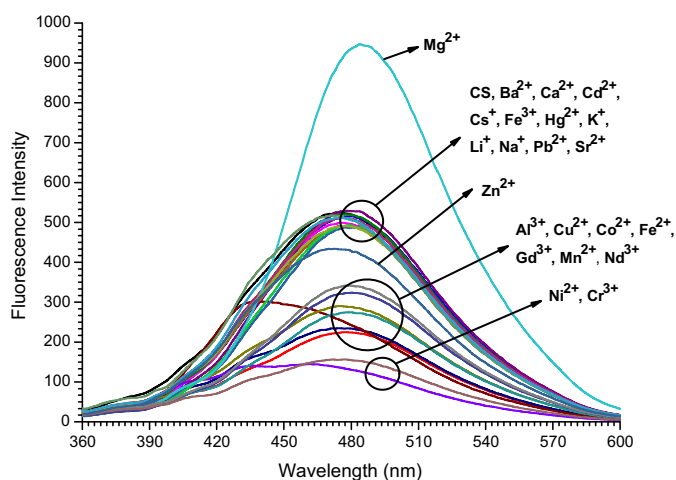


**Fig. 5.** Fluorescence emission spectra ( $\lambda_{\text{ex}} = 340 \text{ nm}$ ) of receptor **CS** (10  $\mu\text{M}$ ) in the presence of 1.0 equiv. of various metal ions in MeOH.

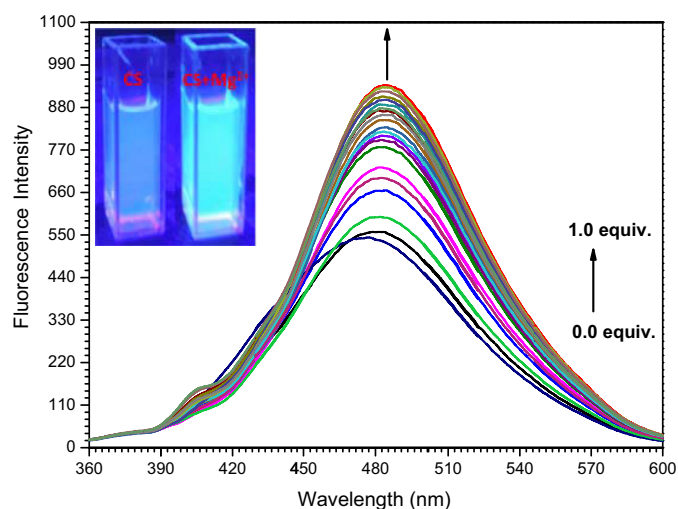


**Fig. 6.** Fluorescent spectral changes of **CS** (10  $\mu\text{M}$ ) upon titration with  $\text{MgCl}_2$  in MeOH. Inset, changes in the fluorescence intensity of **CS** with  $\text{Mg}^{2+}$  under 365 nm UV-light.

any significant spectroscopic change even when added in excess (10 equiv.).

#### 3.2. Fluorescence emission studies

The fluorescence emission spectral behaviour of sensor **CS** (10  $\mu\text{M}$ ) upon addition of various metal ions (10  $\mu\text{M}$ ) has been investigated in methanol. Chemosensor alone showed a single emission band at 473 nm with an excitation of 350 nm. **CS** showed a chelation enhanced fluorescence (CHEF) only with  $\text{Mg}^{2+}$ , even though there was a relatively chelation enhanced fluorescent quenching (CHEQ) effect with  $\text{Al}^{3+}$ ,  $\text{Co}^{2+}$ ,  $\text{Cr}^{3+}$ ,  $\text{Cu}^{2+}$ ,  $\text{Fe}^{2+}$ ,  $\text{Gd}^{3+}$ ,  $\text{Mn}^{2+}$ ,  $\text{Nd}^{3+}$ ,  $\text{Ni}^{2+}$  and  $\text{Zn}^{2+}$  (Fig. 5).

The sequential addition of  $\text{Mg}^{2+}$  ions from 0 to 1.0 equiv. to the solution of **CS** showed a gradual increase in emission accompanied by a small red shift of 12 nm from 473 to 485 nm (Fig. 6). Under a UV lamp, the solution of **CS** in the presence of  $\text{Mg}^{2+}$  showed a dramatic color change from dull fluorescent blue to bright fluorescent blue, which could easily be detected by the naked-eye (Fig. 6, inset). Furthermore, to explore the binding mechanism, the Job's plot of fluorescence emission titration of  $\text{Mg}^{2+}$  was revealed in Fig. 7. A maximum emission was observed when the molar fraction reached

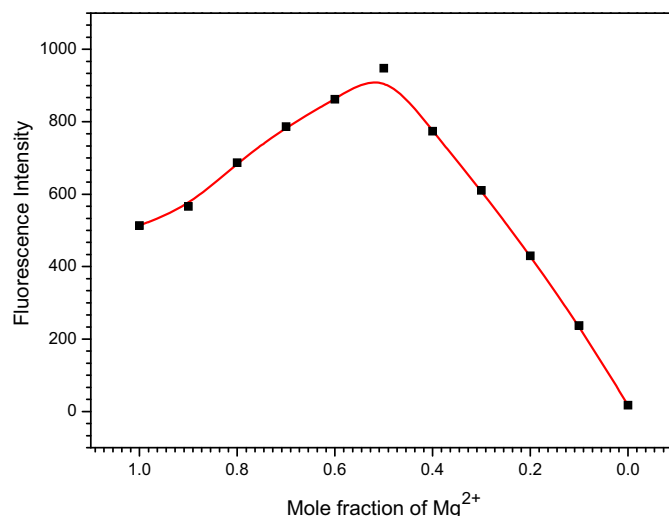


**Fig. 7.** Job's plot, Fluorescence intensity at 485 nm was plotted as a function of the molar ratio.

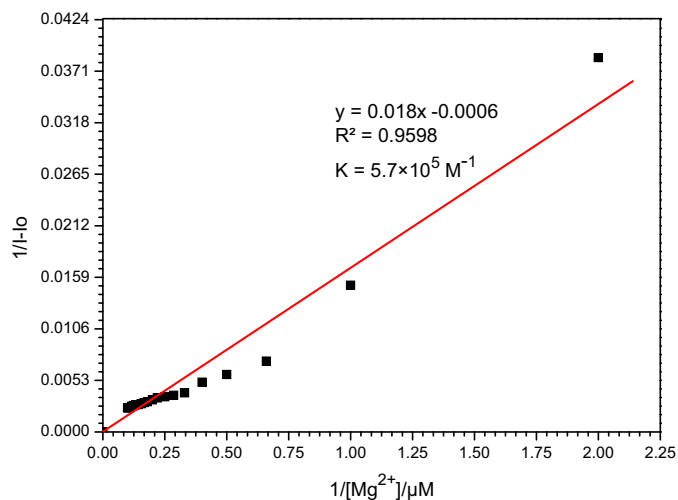


Fig. 8. Benesi-Hildebrand plot, fluorescence intensity at 485 nm.

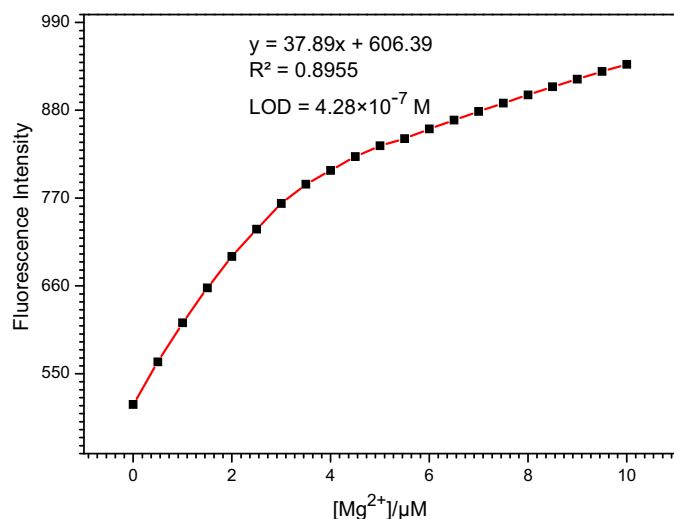


Fig. 9. The linear relation for fluorescent intensity of CS (10  $\mu\text{M}$ ) toward  $\text{Mg}^{2+}$  concentration in the range of 0–10  $\mu\text{M}$ .

0.5, which is indicative of a 1:1 stoichiometry complexation for the newly formed species of  $\text{CS-Mg}^{2+}$ .

From the Fluorescence titration profiles, linear relationship was obtained for the plot measured  $[1/(I - I_0)]$  at 485 nm as a

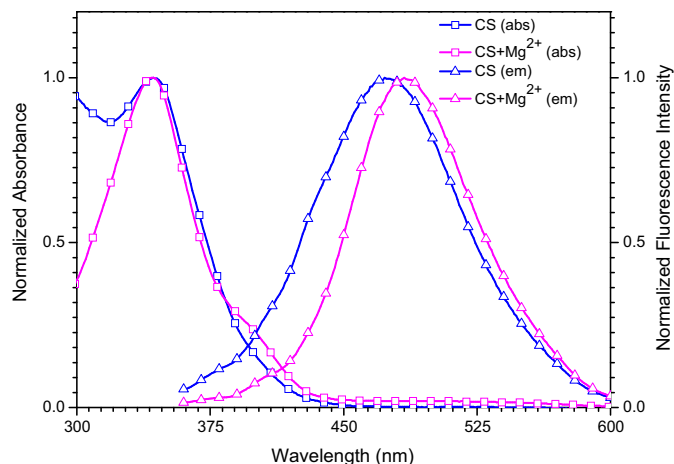


Fig. 11. UV-vis absorption and fluorescence emission spectra of CS and  $\text{CS-Mg}^{2+}$  recorded in methanol.

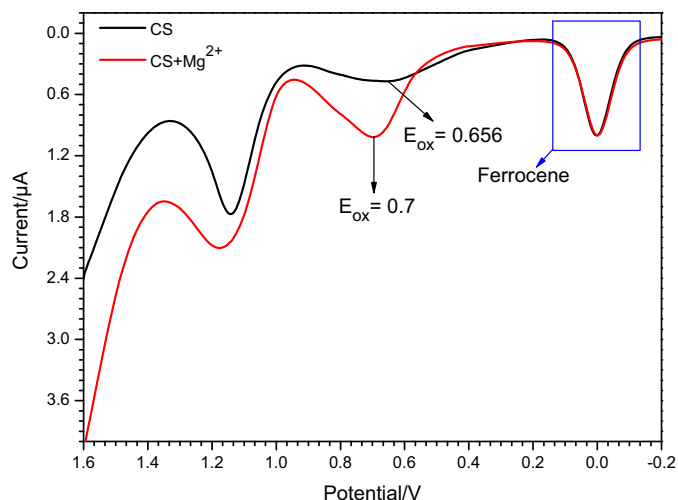


Fig. 12. Differential pulse voltammograms recorded for the probe CS and the corresponding  $\text{Mg}^{2+}$  addition product in methanol.

function of  $1/[\text{Mg}^{2+}]$  using the well-known linear Benesi-Hildebrand expression [30]. The binding constant of the newly formed complex ( $\text{CS-Mg}^{2+}$ ) in MeOH was determined as  $5.7 \times 10^5 \text{ M}^{-1}$  (Fig. 8). The detection limit was calculated based on the fluorescence titration of  $\text{Mg}^{2+}$  as  $0.43 \mu\text{M}$  based on  $S/N = 3$  (Fig. 9).

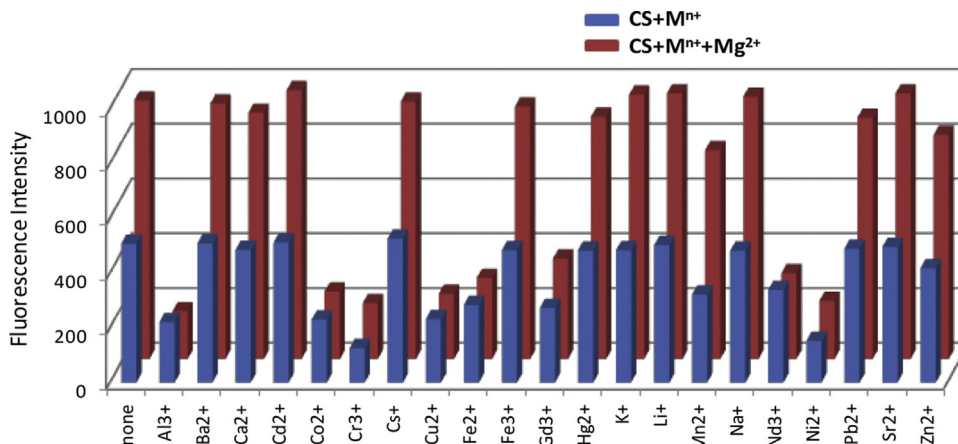


Fig. 10. Selectivity of the probe CS toward various metal ions (1.0 equiv.) in the absence and presence of  $\text{Mg}^{2+}$  (1.0 equiv.), fluorescence intensity at 485 nm.

In addition, the selectivity of **CS** towards  $\text{Mg}^{2+}$  over other metal ions was investigated by the competition experiment. As shown in Fig. 10, probe **CS** ( $10\ \mu\text{M}$ ) was treated with 1 equiv. of  $\text{Mg}^{2+}$  in the presence of other metal ions of the same concentration. Relatively low interference levels were observed for the detection of  $\text{Mg}^{2+}$  in the presence of alkali ( $\text{Li}^+$ ,  $\text{Na}^+$ ,  $\text{K}^+$  and  $\text{Cs}^+$ ), alkaline earth ( $\text{Ca}^{2+}$ ,  $\text{Sr}^{2+}$  and  $\text{Ba}^{2+}$ ), p-block ( $\text{Pb}^{2+}$ ) and d-block ( $\text{Fe}^{3+}$ ,  $\text{Mn}^{2+}$ ,  $\text{Zn}^{2+}$ ,  $\text{Cd}^{2+}$  and  $\text{Hg}^{2+}$ ) metal ions. The receptor **CS** responses for  $\text{Mg}^{2+}$  in the presence of  $\text{Al}^{3+}$ ,  $\text{Co}^{2+}$ ,  $\text{Cr}^{3+}$ ,  $\text{Cu}^{2+}$ ,  $\text{Fe}^{2+}$ ,  $\text{Gd}^{3+}$ ,  $\text{Nd}^{3+}$  and  $\text{Ni}^{2+}$  are relatively low. Thus probe **CS** can be used as a selective fluorescent chemosensor for  $\text{Mg}^{2+}$  in the presence of most competing metal ions especially alkali and alkaline earth metal ions.

### 3.3. Electrochemical measurement

As shown in Fig. 11, the corresponding wavelength to the band gap energy can be calculated from the cross point of absorption and emission onset lines. The corresponding wavelength for **CS** is 396 nm and **CS** +  $\text{Mg}^{2+}$  is 415 nm which are equal to 3.13 eV (for **CS**) and 2.99 eV (for **CS** +  $\text{Mg}^{2+}$ ) band gap energy.

Fig. 12 shows the current–voltage curve for **CS** and **CS** +  $\text{Mg}^{2+}$  regarding to Differential Pulse Voltammetric experiments. Based on results, **CS** shows  $E_{\text{ox}} = 0.656\ \text{V}$  which is equal to  $E_{\text{HOMO}} = -5.46\ \text{eV}$  and **CS** +  $\text{Mg}^{2+}$  shows  $E_{\text{ox}} = 0.7\ \text{V}$  which is equal to  $E_{\text{HOMO}} = -5.5\ \text{eV}$  [31–42]. By addition of  $\text{Mg}^{2+}$  ion increased the oxidation potential of **CS**, due to decrease in electron releasing nature of **CS**– $\text{Mg}^{2+}$  complex. LUMO energy levels (for **CS** is  $-2.33\ \text{eV}$ , for **CS** +  $\text{Mg}^{2+}$  is  $-2.51\ \text{eV}$ ) were estimated from HOMO and band gap energies.

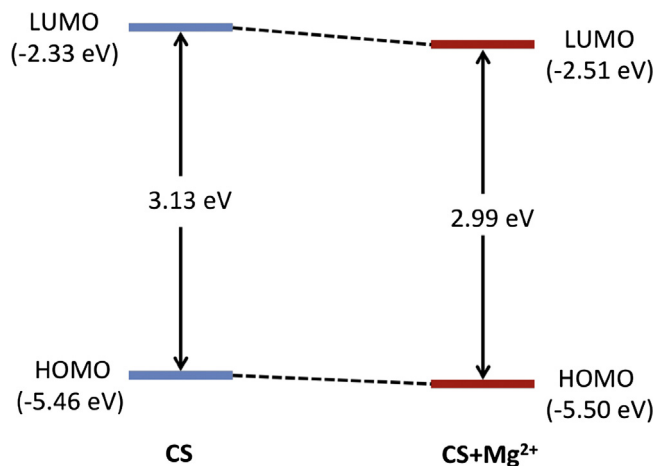


Fig. 13. Energy level diagram of the probe **CS** and the corresponding  $\text{Mg}^{2+}$  addition product.

This experiment proves that, increase in oxidation potential and decrease in band gap due to the interaction between **CS** probe and magnesium ion. Fig. 13 shows the energy diagram with HOMO/LUMO levels of **CS** and **CS** +  $\text{Mg}^{2+}$ .

### 3.4. $^1\text{H}$ NMR titration

To further clarify the bonding mode of sensing probe (**CS**) towards  $\text{Mg}^{2+}$ ,  $^1\text{H}$  NMR titration experiments were carried out in

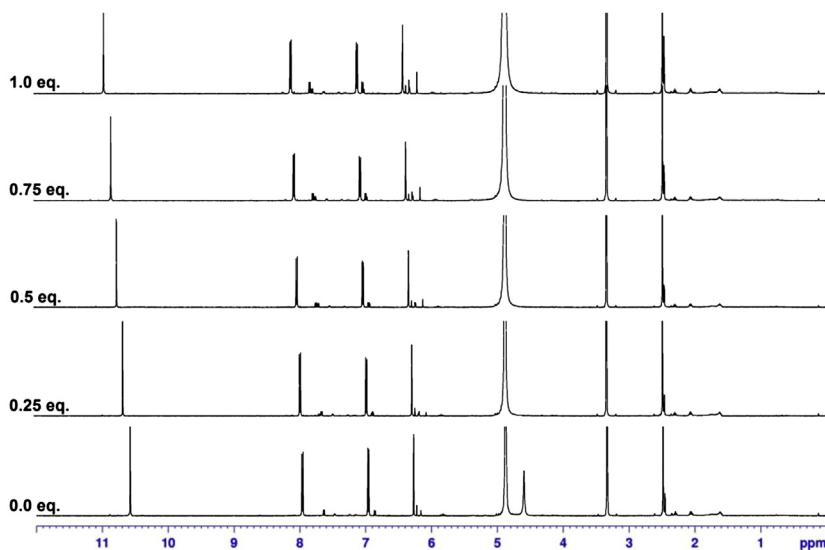
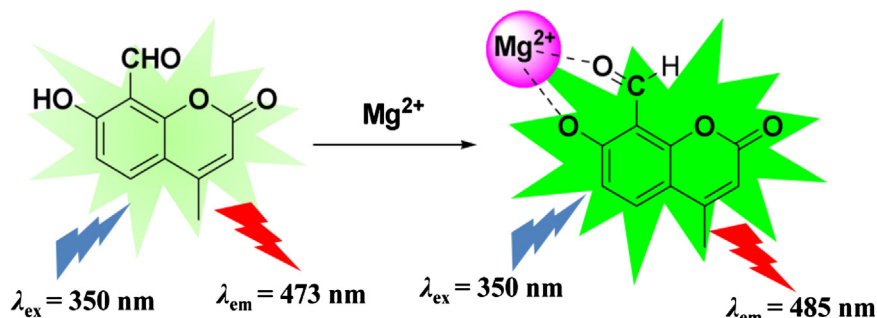
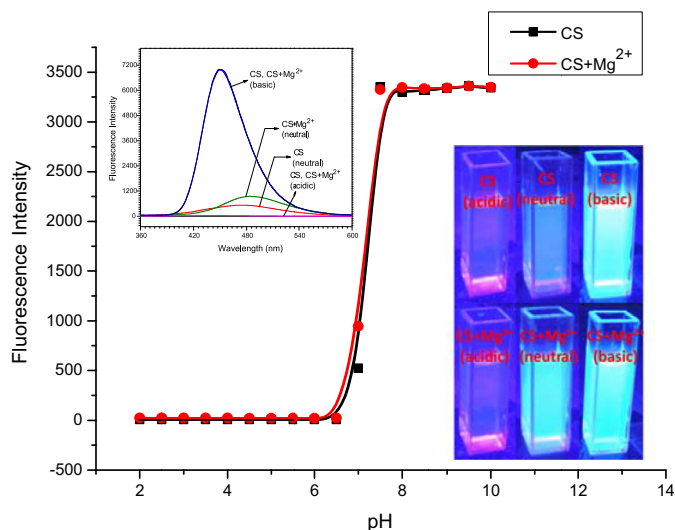


Fig. 14.  $^1\text{H}$  NMR titration plot of receptor **CS** with  $\text{Mg}^{2+}$  in  $\text{CD}_3\text{OD}$ .



Scheme 2. Schematic representation of binding mode of receptor with  $\text{Mg}^{2+}$ .





**Fig. 15.** Fluorescence intensities of **CS** (10  $\mu\text{M}$ ) at 485 nm in the presence of  $\text{Mg}^{2+}$  (10  $\mu\text{M}$ ) under different pH conditions. Inset: Spectral changes of **CS**– $\text{Mg}^{2+}$  as a function of pH (left), photographs of **CS** and **CS**– $\text{Mg}^{2+}$  in different pH media under a UV lamp (right).

both absence and presence of magnesium ion in various concentrations in methanol- $\text{d}_4$  at room temperature. As depicted in Fig. 14, the aldehyde proton of **CS** at around 10.58 ppm was shifted downfield toward 10.98 ppm upon addition of  $\text{Mg}^{2+}$ . The hydroxyl proton was disappeared in  $\text{CD}_3\text{OD}$  solvent. On the other hand, the aromatic protons were shifted downfield by 0.02–0.17 ppm followed the addition of  $\text{Mg}^{2+}$ . The results suggested that the binding of probe (**CS**) to  $\text{Mg}^{2+}$  forms a rigid system by a chelation with the phenolic OH and the oxygen atom of carbonyl group (Scheme 2).

### 3.5. pH effect

The pH-dependent response of **CS** was carried out to investigate a suitable pH range for  $\text{Mg}^{2+}$  sensing. As shown in Fig. 15, the fluorescence emission changes were observed at 485 nm with pH variation. After mixing **CS** with  $\text{Mg}^{2+}$  in the basic pH range, exhibited a rapid fluorescence enhancement accompanied by a blue shift of 37 nm from 485 to 448 nm. The emission intensity of **CS**– $\text{Mg}^{2+}$

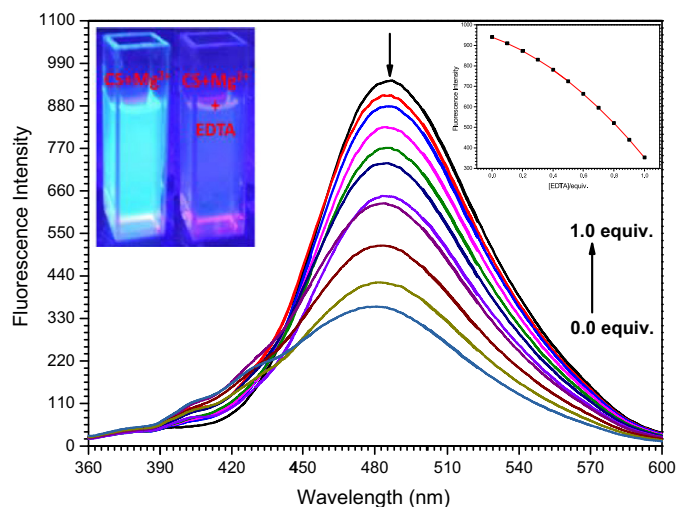


**Fig. 16.** The variation in Fluorescence emission spectra of **CS**– $\text{Mg}^{2+}$  (10  $\mu\text{M}$ ) upon addition of EDTA in methanol. Inset: The color changes of **CS**– $\text{Mg}^{2+}$  upon addition of EDTA (1 equiv.) (left), fluorescence spectral changes at 485 nm as a function of the amount of EDTA (right).

complex was quenched in the acidic conditions. For  $\text{pH} < 7$ , the decreased fluorescence intensity at 485 nm indicates that the protonation of coumarin prevents the formation of **CS**– $\text{Mg}^{2+}$  complexes in acidic condition. The chemosensors **CS** in the presence of  $\text{Mg}^{2+}$  showed a dramatic color changes in the different pH conditions, which could easily be detected by the naked-eye (Fig. 15, inset) under a UV lamp. The same fluorescence emission changes were observed for **CS** alone in acidic and basic conditions.

### 3.6. Reversibility of complexation of probe– $\text{Mg}^{2+}$

To establish the reversibility binding of **CS**– $\text{Mg}^{2+}$ , EDTA titration was conducted. This experiment was performed by the addition of EDTA to the mixture of **CS** (1equiv.) and  $\text{Mg}(\text{II})$  (1equiv.). Therefore, the addition of EDTA to a mixture of receptor **CS** and  $\text{Mg}^{2+}$  resulted in quenching of the fluorescence intensity at 485 nm, which indicated the regeneration of the free receptor **CS** (Fig. 16). The fluorescence was recovered by the addition of  $\text{Mg}^{2+}$  again. These results show that **CS** is suitable to be used as a reversible fluorescent chemosensor to detect  $\text{Mg}^{2+}$ .

## 4. Conclusion

In summary, we have found a coumarin based sensitive probe **CS** to  $\text{Mg}^{2+}$  which fluorometrically selective with  $\text{Mg}^{2+}$  ions and makes it a dual probe for naked eye detection of  $\text{Mg}^{2+}$  through change in color and fluorescence. The limit of detection of  $\text{Mg}^{2+}$  was found to be much lower as 0.43  $\mu\text{M}$ . The binding ability and mode of sensor **CS** towards  $\text{Mg}^{2+}$  were investigated through UV–vis absorption, fluorescence emission, electrochemical and  $^1\text{H}$  NMR spectroscopic techniques. Thus, our chemosensor can be used as a practical sensor for detection of  $\text{Mg}^{2+}$  in analytical as well as environmental and biological samples.

## Acknowledgements

One of the authors (Naveen) is grateful to the Ministry of Human resource and Development (MHRD), New Delhi, India for financial support.

## References

- [1] R.D. Grubbs, M.E. Maguire, Magnesium as a regulatory cation: criteria and evaluation, *Magnesium* 6 (1987) 113–127.
- [2] R. Bogoroch, L.F. Belanger, Skeletal effects of magnesium deficiency in normal, ovariectomized, and estrogen-treated rats, *Anat. Rec.* 183 (1975) 437–447.
- [3] H.O. Trowbridge, J.L. Seltzer, Formation of dentin and bone matrix in magnesium-deficient rats, *J. Periodontol. Res.* 2 (1967) 147–153.
- [4] M.E. Maguire, J.A. Cowan, Magnesium chemistry and biochemistry, *Biomaterials* 15 (2002) 203–210.
- [5] R. Swaminathan, Magnesium metabolism and its disorders, *Clin. Biochem. Rev.* 24 (2003) 47–66.
- [6] W. Jahnhen-Dechent, M. Ketteler, Magnesium basics, *Clin. Kidney J.* 5 (2012) i3–i14.
- [7] L. Fabbri, A. Poggi, Sensors and switches from supramolecular chemistry, *Chem. Soc. Rev.* 24 (1995) 197–202.
- [8] B. Valeur, I. Leray, Design principles of fluorescent molecular sensors for cation recognition, *Coord. Chem. Rev.* 205 (2000) 3–40.
- [9] S.L. Wiskur, H. Ait-Haddou, J.J. Lavigne, E.V. Anslyn, Teaching old indicators new tricks, *Acc. Chem. Res.* 34 (2001) 963–972.
- [10] K. Rurack, U. Resch-Genger, Rigidization, preorientation and electronic decoupling—the ‘magic triangle’ for the design of highly efficient fluorescent sensors and switches, *Chem. Soc. Rev.* 31 (2002) 116–127.
- [11] G.W. Gokel, W.M. Leevy, M.E. Weber, Crown ethers: sensors for ions and molecular scaffolds for materials and biological models, *Chem. Rev.* 104 (2004) 2723–2750.
- [12] A.P. de Silva, H.Q.N. Gunaratne, T. Gunnlaugsson, A.J.M. Huxley, C.P. McCoy, J.T. Rademacher, T.E. Rice, Signaling recognition events with fluorescent sensors and switches, *Chem. Rev.* 97 (1997) 1515–1566.
- [13] V.K. Gupta, A.K. Singh, L.K. Kumawat, Thiazole schiff base turn-on fluorescent chemosensor for  $\text{Al}^{3+}$  ion, *Sens. Actuators B* 195 (2014) 98–108.
- [14] V.K. Gupta, A.K. Singh, N. Mergu, Antipyrine based schiff bases as turn-on fluorescent sensors for  $\text{Al}(\text{III})$  ion, *Electrochim. Acta* 117 (2014) 405–412.

- [15] V.K. Gupta, N. Mergu, A.K. Singh, Fluorescent chemosensors for  $Zn^{2+}$  ions based on flavonol derivatives, *Sens. Actuators B* 202 (2014) 674–682.
- [16] D. Kand, A.M. Kalle, S.J. Varma, P. Talukdar, A chromenoquinoline-based fluorescent off-on thiol probe for bioimaging, *Chem. Commun.* 48 (2012) 2722–2724.
- [17] G. Zhang, Y. Wen, C. Guo, J. Xu, B. Lu, X. Duan, H. He, J. Yang, A cost-effective and practical polybenzanthrone-based fluorescent sensor for efficient determination of palladium (II) ion and its application in agricultural crops and environment, *Anal. Chim. Acta* 805 (2013) 87–94.
- [18] G. Farruggia, S. Iotti, L. Prodi, M. Montalti, N. Zaccaroni, P.B. Savage, V. Trapani, P. Sale, F.I. Wolf, 8-hydroxyquinoline derivatives as fluorescent sensors for magnesium in living cells, *J. Am. Chem. Soc.* 128 (2006) 344–350.
- [19] H. Hama, T. Morozumi, H. Nakamura, Novel  $Mg^{2+}$ -responsive fluorescent chemosensor based on benzo-15-crown-5 possessing 1-naphthaleneacetamide moiety, *Tetrahedron Lett.* 48 (2007) 1859–1861.
- [20] K.C. Song, M.G. Choi, D.H. Ryu, K.N. Kim, S.K. Chang, Ratiometric chemosensing of  $Mg^{2+}$  ions by a calix[4]arene diamide derivative, *Tetrahedron Lett.* 48 (2007) 5397–5400.
- [21] H.M. Kim, P.R. Yang, M.S. Seo, J.S. Yi, J.H. Hong, S.J. Jeon, Y.G. Ko, K.J. Lee, B.R. Cho, Magnesium ion selective two-photon fluorescent probe based on a benzo[h]chromene derivative for in vivo imaging, *J. Org. Chem.* 27 (2007) 2088–2096.
- [22] Y. Liu, Z.Y. Duan, H.Y. Zhang, X.L. Jiang, J.R. Han, Selective binding and inverse fluorescent behavior of magnesium ion by podand possessing plural imidazo[4,5-f]-1,10-phenanthroline groups and its  $Ru(II)$  complex, *J. Org. Chem.* 70 (2005) 1450–1455.
- [23] B.J. Sanghavi, W. Varhue, J.L. Chavez, C.F. Chou, N.S. Swami, Electrokinetic preconcentration and detection of neuropeptides at patterned graphene-modified electrodes in a nanochannel, *Anal. Chem.* 86 (2014) 4120–4125.
- [24] B.J. Sanghavi, S. Sitaula, M.H. Griep, S.P. Karna, M.F. Ali, N.S. Swami, Real-time electrochemical monitoring of adenosine triphosphate in the picomolar to micromolar range using graphene-modified electrodes, *Anal. Chem.* 85 (2013) 8158–8165.
- [25] B.J. Sanghavi, S.M. Mobin, P. Mathur, G.K. Lahiri, A.K. Srivastava, Biomimetic sensor for certain catecholamines employing copper(II) complex and silver nanoparticle modified glassy carbon paste electrode, *Biosens. Bioelectron.* 39 (2013) 124–132.
- [26] B.J. Sanghavi, A.K. Srivastava, Simultaneous voltammetric determination of acetaminophen, aspirin and caffeine using an in situ surfactant-modified multiwalled carbon nanotube paste electrode, *Electrochim. Acta* 55 (2010) 8638–8648.
- [27] B.J. Sanghavi, A.K. Srivastava, Adsorptive stripping differential pulse voltammetric determination of venlafaxine and desvenlafaxine employing nafion-carbon nanotube composite glassy carbon electrode, *Electrochim. Acta* 56 (2011) 4188–4196.
- [28] H. Pechmann, C. Duisberg, Über die verbindungen der phenole mit acetessigäther, *Ber. Dtsch. Chem. Ges.* 16 (1883) 2119–2128.
- [29] A.D. Patel, M.S. Sharma, J.J. Vora, J.D. Joshi, Synthesis, characterization and antimicrobial activities of binary and ternary complexes of  $UO_2^{2+}$  and  $ThIV$  complexes with 5-hydroxymethyl-8-quinolinol and 8-formyl-7-hydroxy-4-methyl-2H-1-benzopyran-2-one with aniline, *J. Indian Chem. Soc.* 74 (1997) 287–288.
- [30] H.A. Benesi, J.H. Hildebrand, A spectrophotometric investigation of the interaction of iodine with aromatic hydrocarbons, *J. Am. Chem. Soc.* 71 (1949) 2703–2707.
- [31] J.L. Bredas, R. Silbey, D.S. Boudreau, R.R. Chance, Chain-length dependence of electronic and electrochemical properties of conjugated systems: polyacetylene, polyphenylene, polythiophene, and polypyrrole, *J. Am. Chem. Soc.* 105 (1983) 6555–6559.
- [32] V.K. Gupta, A.K. Jain, G. Maheshwari, Novel Aluminum (III) selective potentiometric sensor based on morin in poly (vinyl chloride) matrix, *Talanta* 72 (4) (2007) 1469–1473.
- [33] V.K. Gupta, M.R. Ganjali, P. Norouzi, H. Khani, A. Nayak, S. Agarwal, Electrochemical analysis of some toxic metals and drugs by ion selective electrodes, *Crit. Rev. Anal. Chem.* 41 (2011) 282–313.
- [34] R.N. Goyal, V.K. Gupta, S. Chatterjee, Voltammetric biosensors for the determination of paracetamol at carbon nanotube modified pyrolytic graphite electrode, *Sens. Actuators B, Chem.* 149 (2010) 252–258.
- [35] V.K. Gupta, A.K. Jain, Shiva Agarwal, G. Maheshwari, An iron (III) ion-selective sensor based on a (bis (tridentate) ligand, *Talanta* 71 (2007) 1964–1968.
- [36] R. Jain, V.K. Gupta, N. Jadon, K. Radhapyari, Voltammetric determination of Cefixime in pharmaceuticals and biological fluids, *Anal. Biochem.* 407 (2010) 79–88.
- [37] V.K. Gupta, A.K. Singh, S. Mehtab, B. Gupta, ACobalt (II) selective PVC membrane based on a Schiff base complex of N, N'-bis (salicylidene)-3,4-diaminotoluene, *Anal. Chim. Acta* 566 (2006) 5–10.
- [38] R.N. Goyal, V.K. Gupta, S. Chatterjee, Electrochemical oxidation of 2', 3'-dideoxyadenosine at pyrolytic graphite electrode, *Electrochim. Acta* 53 (2008) 5354–5360.
- [39] V.K. Gupta, A.K. Singh, M. Al Khayat, B. Gupta, Neutral carriers based poly431 meric membrane electrodes for selective determination of Mercury (II), *Anal. Chim. Acta* 590 (2007) 81–90.
- [40] V.K. Gupta, R. Prasad, R. Mangla, P. Kumar, New nickel (II) selective potentiometric sensor based on 5,12,14-tetramethyldibenzotetraazaannulene in a poly (vinyl chloride) matrix, *Anal. Chim. Acta* 420 (2000) 19–27.
- [41] R.N. Goyal, V.K. Gupta, S. Chatterjee, Simultaneous determination of adenosine and inosine using single-wall carbon nanotubes modified pyrolytic graphite electrode, *Talanta* 76 (2008) 662–668.
- [42] V.K. Gupta, I. Ali, T.A. Saleh, A. Nayak, S. Agarwal, Chemical treatment technologies for wastewater recycling—a review, *RSC Adv.* 2 (2012) 6380–6388.

## Bioographies



**Vinod Kumar Gupta** obtained his PhD degree in chemistry from the University of Roorkee (now Indian Institute of Technology Roorkee) Roorkee, India, in 1979. Since then he is pursuing research at the same Institute and presently holding the position of Professor of Chemistry Department, at Indian Institute of Technology Roorkee, Roorkee. He worked as a post-doctoral fellow at University of Regensburg, Germany, in 1993 as an EC fellow and was DAAD visiting professor at University of Chemnitz and Freie University of Berlin in 2002. He has published more than 400 paper with h-index of 110 and citation > 27000. His research interests include chemical sensors, waste water treatment, environmental and electro analytical chemistry. Dr. Gupta is an elected Fellow of the World Innovation Foundation (FIWF) since July 2004 and Fellow of the National Academy of Sciences (FNASc) since 2008.



**Naveen Mergu**, is a PhD student and pursuing research on chemical sensors under the supervision of V.K. Gupta and A.K. Singh at IIT Roorkee. He did his M.Sc. in 2010 in Chemistry at NIT Warangal.



**Lokesh Kumar Kumawat** is a Ph.D student and persuing research on chemical sensor under the supervision of V.K. Gupta and A. K. Singh at IIT Roorkee. He has completed his master degree in chemistry from MLSU (Mohan Lal Sukhadia University) Udaipur, India in 2009



**Ashok Kumar Singh** is in teaching and research profession for almost 30 years. Presently, he is a Professor of Chemistry at Indian Institute of Technology Roorkee, India and has more than 150 research publications to his credit. Prof. Singh works extensively in the field of macrocyclic chemistry